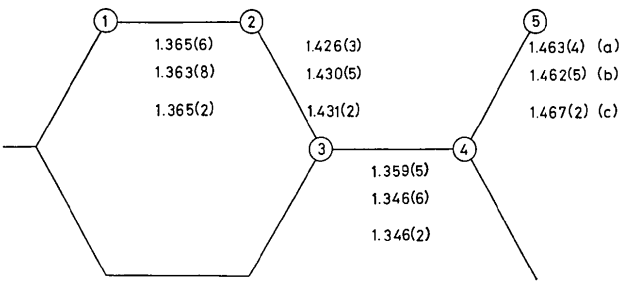

Fig. 4. Bond lengths observed in (*a*) TMPD.ClO_4(RT), (*b*) TMPD iodide and (*c*) TMPD.ClO_4(LT). The values are corrected for libration.

References

BOER, J. L. DE, VOS, A. & HUML, K. (1968). *Acta Cryst.* B**24**, 542.

BOER, J. L. DE (1970). Thesis, Groningen.

BOER, J. L. DE & VOS, A. (1972). *Acta Cryst.* B**28**, 839.

BUSING, W. R. & LEVY, H. A. (1957). *Acta Cryst.* **10**, 180.

CHU, T. L., PAKE, G. E., PAUL, D. E., TOWNSEND, J. & WEISSMAN, S. I. (1953). *J. Phys. Chem.* **57**, 504.

CRUICKSHANK, D. W. J. (1956). *Acta Cryst.* **9**, 754.

CRUICKSHANK, D. W. J. (1961). *Computing Methods and the Phase Problem in X-ray Crystal Analysis.* London: Pergamon Press.

MICHAELIS, L. & GRANICK, S. (1943). *J. Amer. Chem. Soc.* **65**, 1747.

MONKHORST, H. J., POTT, G. T. & KOMMANDEUR, J. (1967). *J. Chem. Phys.* **47**, 401.

MOORE, F. H. (1963). *Acta Cryst.* **16**, 1169.

PARISER, R. & PARR, R. G. (1953). *J. Chem. Phys.* **21**, 466, 767.

POPLE, J. A. (1953). *Trans. Faraday Soc.* **49**, 1375.

POTT, G. T. (1966). Thesis, Groningen.

POTT, G. T., VAN BRUGGEN, C. F. & KOMMANDEUR, J. (1967). *J. Chem. Phys.* **47**, 408.

POTT, G. T. & KOMMANDEUR, J. (1967). *J. Chem. Phys.* **47**, 395.

SOOS, Z. G. (1965). *J. Chem. Phys.* **43**, 1121.

SOOS, Z. G. & HUGHES, R. C. (1967). *J. Chem. Phys.* **46**, 253.

STEWART, R. F., DAVIDSON, E. R. & SIMPSON, W. T. (1965). *J. Chem. Phys.* **42**, 3175.

THOMAS, D. D., KELLER, H. & MCCONNELL, H. M. (1963). *J. Chem. Phys.* **39**, 2321.

Acta Cryst. (1972). B**28**, 839

The Crystal Structure of the Room- and Low-Temperature Modifications of Wurster's Blue Perchlorate, TMPD. ClO_4. II. The Low-Temperature Phase

BY J. L. DE BOER AND AAFJE VOS

Laboratorium voor Structuurchemie, Rijksuniversiteit Groningen, Zernikelaan, Paddepoel, Groningen, The Netherlands

(*Received* 27 *May* 1971)

Crystals of the low-temperature modification of *N,N,N′,N′*-tetramethyl-*p*-diaminobenzene perchlorate (TMPD.ClO_4) have monoclinic symmetry. The crystal structure is described in space group $B2_1/d$. The unit-cell data (in $B2_1/d$) are at 110°K: $a=11{\cdot}655$ (7), $b=10{\cdot}147$ (8), $c=20{\cdot}130$ (10) Å, $\beta=92{\cdot}57$ (2)°, $Z=8$. The *a* and *c* axes are almost doubled in length compared with those of the orthorhombic modification, space group *Pnnm*, existing above the transition point of 186°K. The mirror plane and twofold axis which vanish when going from *Pnnm* to $B2_1/d$ are preserved as twinning elements. Because of the twinning, difficulties were encountered during the intensity measurements. For two different crystals it appeared to be possible, however, to obtain reliable intensities for 3014 and 2737 independent reflexions respectively. The corresponding indices *R* are 0·093 and 0·103. The TMPD groups are arranged in rows, the distances between the benzene planes are alternately 3·10 and 3·62 Å. The bond lengths show that the TMPD groups are present as $TMPD^+$. This rules out the 'mol-ionic' lattice theory of Pott & Kommandeur. The magnetic behaviour of TMPD.ClO_4(LT) can be explained by the theory of Soos based on exchange interaction.

Introduction

In the previous paper (de Boer & Vos, 1972; to be referred to as dBV), the room-temperature (RT) modification of TMPD.ClO_4 is described. The crystals of the RT form are orthorhombic, space group *Pnnm*. When cooling the crystals of TMPD.ClO_4 below the transition point of 186°K, the symmetry is lowered from orthorhombic to monoclinic (Thomas, Keller & McConnell, 1963), and twinning of the crystals is observed. The present paper deals with the low-temperature study of TMPD.ClO_4, the comparison with the RT form, and the discussion of the magnetic properties.

Experimental

Preliminary work, twinning

A preliminary study of the change in symmetry of the crystals during the phase transition was made by use of Weissenberg photographs. The crystals were cooled in a stream of cold nitrogen gas. The Weissenberg pictures showed that the LT form belongs to the monoclinic space group $P2_1/c$. Moreover it was observed that in most cases quadruplets are obtained. To compare the LT form of TMPD.ClO_4 with the RT form, the LT modification can be described best in the centred space group $B2_1/d$ rather than in the non-centred group $P2_1/c$. The mirror plane (001) and the twofold axis [001] of the RT form which are not present in the LT space group, are preserved as twinning elements in the LT crystals. In the observed quadruplets twinning across (001) is present to a considerably larger extent than twinning around [001]. The relative orientation of the four individuals is given in Fig. 1. In the LT modification the a and the c axes are approximately twice as long as in the RT form (see also Thomas *et al.* (1963); in their Fig. 2. II the translation component of the glide plane d should be along their direction [1$\bar{1}$0] rather than along [110]).

Preparation of the crystals

For the determination of the cell dimensions and the collection of the intensities, use was made of an automatic three-circle Nonius diffractometer. The crystals were again cooled in a stream of cold nitrogen gas (for equipment used, see van Bolhuis, 1971). In addition to the quadruplet formation we observed a strong increase in mosaic spread when cooling the crystals below the transition point. It was therefore difficult to obtain good crystal specimens for the intensity measurements. It appeared to be of great help to observe

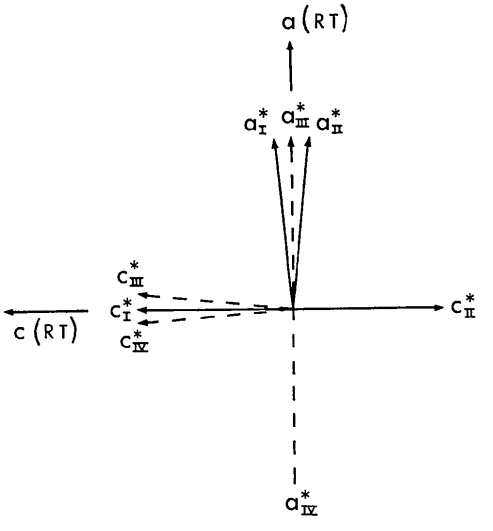

Fig. 1. Relative orientation of the individuals in a quadruplet. Except for individual IV, **b*** points downwards. The deviation of β from 90° is exaggerated by a factor of 2.

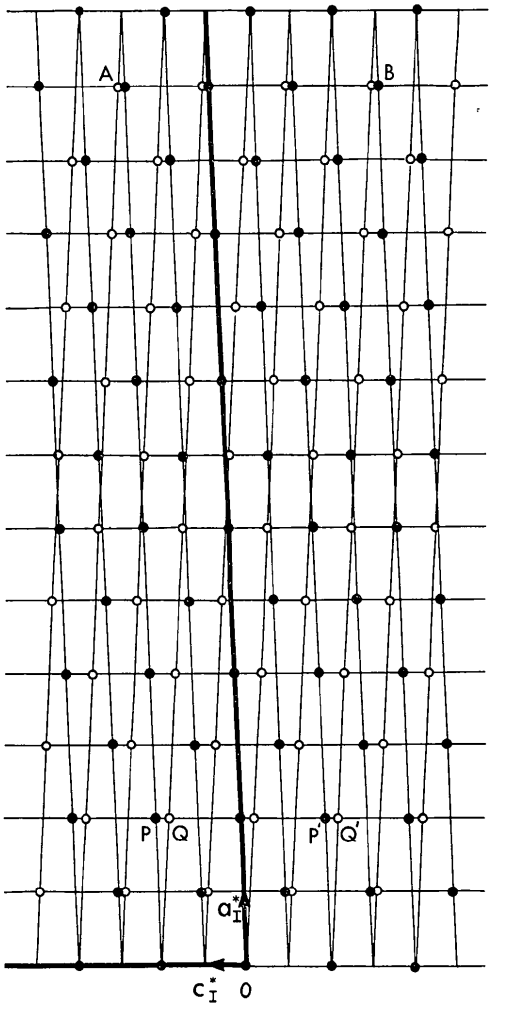

Fig. 2. k-level of reciprocal lattice for a crystal twinned about the RT mirror plane. **b*** points downwards. The reflexions of the individuals I and II are represented by ● and ○ respectively.

that the presence of individuals III and IV could largely be suppressed by cooling the crystals rapidly. After many attempts we obtained two crystals with a negligible amount of individuals III and IV and with a reasonably small, although anisotropic, mosaic spread (maximal 1·7 and 1·2° for crystals 1 and 2 respectively). These crystals were used for the intensity measurements. The arrangement of the reflexions of the twinned crystals in reciprocal space is shown in Fig. 2. In order to minimize overlap effects for neighbouring reflexions (see under intensity measurements), the crystals were mounted along **b**.

Crystal data

The cell constants were determined at 110°K. For space group $B2_1/d$ the values are $a=11{\cdot}655$ (7), $b=10{\cdot}147$ (8), $c=20{\cdot}130$ (10) Å, $\beta=92{\cdot}57$ (2)°. The density of the crystals at 110°K is 4·2% higher than at room temperature. The systematic absences for

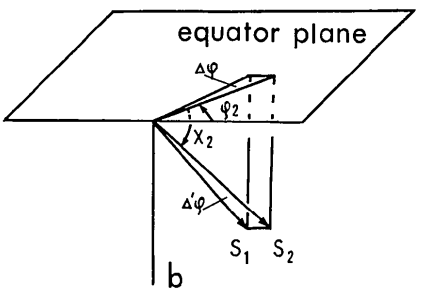

Fig. 3. Difference in ω for two 'neighbouring' reflexions. The difference in length of S_1 and S_2 gives $(\Delta\omega)' = \theta_2 - \theta_1$. In addition to this there is a ω difference of $(\Delta\omega)'' = \Delta'\varphi \simeq (\varphi_2 - \varphi_1) \cos \frac{1}{2}(\chi_2 + \chi_1)$, where χ_1 and χ_2 are the χ values of the two reflexions.

$B2_1/d$ are: hkl absent for $h+l \neq 2n$, $h0l$ absent for $h+l \neq 4n$ and $0k0$ absent for $k \neq 2n$, the latter relation was verified by using different mountings of the crystal and Cu as well as Mo radiation.

Intensity measurements

The intensity measurements were made at 110°K. For each twin of the two crystals used, all independent reflexions with $\sin\theta/\lambda \leq 0{\cdot}746$ Å^{-1} were measured with Zr-filtered Mo radiation. In view of the magnitude of the mosaic spread of the crystals, the ω-scan technique was applied.

When processing the data it had to be decided whether or not the intensities obtained for two neighbouring reflexions (say P and Q in Fig. 2) were in error owing to overlap effects. To this end we calculated the reflection distance $g = \theta_2 - \theta_1 + [\varphi_2(b) - \varphi_1(b)] \cos\chi$ (see Fig. 3). For $|g|$ larger than the scanning angle, the reflexions were considered as free. For the free reflexions, the factor $K = \sum I(hkl;\mathrm{I}) / \sum I(hkl;\mathrm{II})$ was calculated (summation over intensities measured for both twin individuals). The factor appeared to be approximately the same for the two crystals considered, *viz.* 0·774 for 1 and 0·794 for 2.

The non-interfering reflexions were further used to determine the heights of the backgrounds as a function of θ. This information is essential for the analysis of a second series of reflexions. This series is composed of pairs of reflexions for which the peak position (M) of one of the reflexions (P say) coincides with a background position of the other (Q say). The intensity measured at M is thus $I(M) = I(\text{peak } P) + I(\text{background } Q)$. For $I(M)$ equal to the expected value for the background of Q, within experimental error, the reflexion P was considered as unobservable and the intensity measured for Q could be regarded as being undisturbed by P.

Finally the intensities could be calculated for completely or nearly completely coinciding reflexions. This can be understood as follows. At the positions A and B in Fig. 2 are obtained the intensities $I(A) = I(hkl_1;\mathrm{I}) + I(hkl_2;\mathrm{II}) = I(hkl_1;\mathrm{I}) + I(hkl_2;\mathrm{I})/K$ and $I(B) = I(hkl_1;\mathrm{I})/K + I(hkl_2;\mathrm{I})$. From $I(A)$ and $I(B)$ both $I(hkl_1;\mathrm{I})$ and $I(hkl_2;\mathrm{I})$ can be calculated owing to the fact that the factor K is not unity. When the coinciding reflexions are equivalent, as is for instance the case for the reflexion pair $(0kl;\mathrm{I})$ and $(0k\bar{l};\mathrm{II})$, measurement of $I(B)$ has been omitted and the intensity $I(hkl_1;\mathrm{I}) = I(hkl_2;\mathrm{I})$ is obtained from the equation $I(hkl_1;\mathrm{I}) = I(A)\,K/(K+1)$.

Processing of the data by the methods described above gave 2737 reliable intensities for crystal 1 and 3014 reliable intensities for crystal 2. The explored part of the reciprocal space contained approximately 4100 independent reflexions. When calculating F_o values from the collected intensities, Lorentz and polarization effects were taken into account; no absorption corrections were applied.

Structure determination

As mentioned above, the a and c axes of the B-centred cell of the LT form are approximately twice as long as the corresponding axes of the primitive cell of the RT form. Because of this the LT reflexions may be separated into two groups. First, the reflexions with h (and therefore also l) even ('even' reflexions) which are observed also for the RT form, and secondly the reflexions with h and l odd ('uneven' reflexions) which do not occur at room temperature. We observed that the intensities of the even reflexions are, on the average,

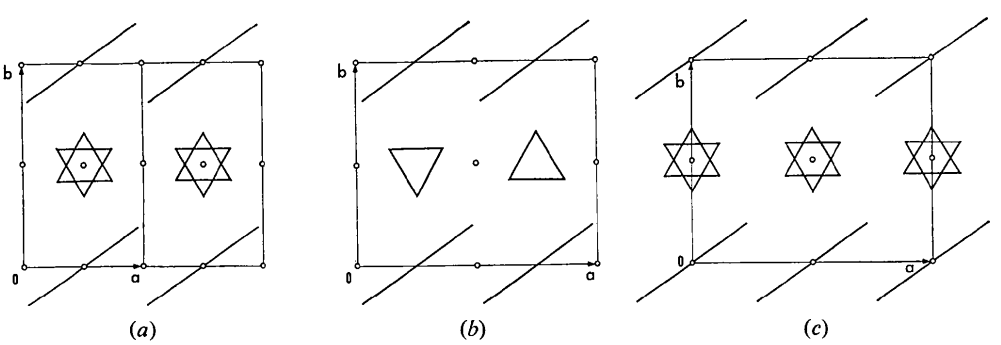

Fig. 4. The RT structure (a) and the two models derived from it for the LT structure ($b+c$). Only ions lying athwart $z=0$ are given. TMPD groups are represented by straight lines and ClO_4 groups by triangles. Intersecting triangles indicate disorder of the ClO_4 groups.

a factor 3 larger than those of the uneven reflexions; moreover the even reflexions appeared to show a reasonable similarity with the data of the RT modification. From this information we concluded that the LT and RT structures are fairly similar and that only moderate atomic displacements accompany the phase transition.

Fig. 4(*a*) shows that at room temperature the inversion centres in the **a** direction are occupied alternately by TMPD groups. In the LT form where the *a* axis is twice as long as in the RT form, one half of the inversion centres is missing and it had to be decided whether the occupied or the free centres disappear during the phase transition. In the first case the eight TMPD groups in the unit cell of the LT form lie at general positions, so that there is only one independent group in the cell [Fig. 4(*b*)]. In the second case the TMPD (and also the ClO_4) groups lie at inversion centres,

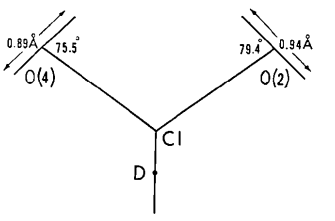

Fig. 5. Projection of the ClO_4 group onto the O(2)–Cl–O(4) plane. *P*[O(2)] and *P*[O(4)] make angles of 18·4 and 1·7° respectively with this plane, their angles with the respective Cl–O bonds are indicated in the Figure.

which implies that the cell contains two independent centrosymmetric TMPD groups and that the ClO_4 groups are disordered [Fig. 4(*c*)]. Structure-factor calculations showed the model of Fig. 4(*b*) to be presumably correct, which was subsequently confirmed during the refinement of the structure.

In the model of Fig. 4(*b*) the centre of the independent TMPD group is placed at ($\frac{1}{4}$00), by analogy with the RT structure. To check how far in the LT form the TMPD group is shifted from this position, an anisotropic least-squares refinement [minimization of $\sum(F_o - kF_c)^2$] was done with the even reflexions. The RT parameters were used as a starting point. From the large U_{11} values obtained for both N and C, we concluded that the TMPD group as a whole had to be shifted some 0·3 Å along **a**. A structure-factor calculation including both the even and uneven reflexions showed that the TMPD group at ($\frac{1}{4}$00) had to be shifted towards ($\frac{1}{2}$00). Further refinement could be done in a routine way. The positions of all independent H atoms could be found from a difference Fourier map, and their parameters were refined isotropically. The scattering factors for hydrogen were taken from Stewart, Davidson & Simpson (1965), and those of the other atoms from Doyle & Turner (1968). Independent refinements were done for crystal 2 and crystal 1. All

Table 1. *Final parameters*

(*a*) Coordinates *x*, *y*, *z* obtained for crystal 2 with calculated standard deviations, and average values x_a, y_a, z_a of the coordinates obtained for crystals 1 and 2. All values are multiplied by 10^4.

	x	*y*	*z*	x_a	y_a	z_a
Cl	7534 (1)	5088 (1)	−46 (1)	7534	5087	−46
C(1)	3086 (3)	487 (3)	705 (1)	3087	487	704
C(2)	2259 (3)	−500 (3)	−520 (2)	2258	−501	−519
C(3)	3202 (3)	291 (3)	−494 (2)	3203	290	−495
C(4)	2129 (3)	−294 (3)	680 (2)	2130	−292	682
C(5)	3655 (2)	835 (3)	117 (2)	3656	835	117
C(6)	1667 (3)	−813 (3)	66 (2)	1668	−815	67
C(7)	4960 (3)	2286 (4)	763 (2)	4957	2291	764
C(8)	287 (3)	−2188 (4)	−578 (2)	287	−2190	−578
C(9)	5043 (3)	2208 (4)	−455 (2)	5042	2207	−455
C(10)	118 (3)	−1893 (4)	645 (2)	116	−1893	645
N(1)	4567 (2)	1653 (3)	144 (1)	4567	1653	143
N(2)	711 (2)	−1553 (3)	42 (1)	710	−1553	41
O(1)	7631 (3)	6465 (3)	76 (2)	7631	6464	76
O(2)	8557 (5)	4633 (5)	−323 (3)	8554	4631	−323
O(3)	7345 (3)	4390 (4)	561 (1)	7345	4394	561
O(4)	6572 (5)	4903 (5)	−504 (2)	6567	4904	−503

Table 1 (*cont.*)

(*b*) Final thermal parameters U_{ij}(in 10^{-4} Å^2) for crystal 2. The temperature factor is $\exp[-2\pi^2(h^2a^{*2}U_{11} + \ldots + 2ha^*kb^*U_{12} + \ldots)]$

	U_{11}	U_{22}	U_{33}	$2U_{12}$	$2U_{23}$	$2U_{13}$
Cl	322 (4)	173 (3)	145 (3)	−20 (6)	11 (5)	46 (5)
C(1)	199 (13)	156 (12)	128 (12)	20 (20)	−26 (20)	25 (19)
C(2)	175 (13)	212 (14)	131 (12)	6 (21)	−54 (21)	2 (19)
C(3)	168 (13)	195 (14)	128 (12)	0 (20)	63 (20)	6 (18)
C(4)	188 (13)	162 (13)	150 (12)	−5 (20)	−14 (20)	45 (19)
C(5)	144 (13)	161 (12)	166 (12)	17 (19)	14 (20)	0 (18)
C(6)	158 (13)	165 (13)	154 (12)	16 (19)	24 (20)	11 (18)
C(7)	256 (16)	259 (16)	197 (14)	−95 (25)	−113 (25)	−25 (22)
C(8)	234 (15)	285 (17)	232 (15)	−144 (25)	−73 (26)	−13 (23)
C(9)	235 (15)	267 (16)	205 (14)	−75 (24)	66 (25)	63 (22)
C(10)	229 (15)	295 (17)	230 (15)	−120 (25)	18 (26)	103 (23)
N(1)	187 (12)	164 (11)	160 (11)	−40 (18)	2 (19)	−10 (17)
N(2)	183 (12)	191 (12)	161 (11)	7 (18)	17 (19)	33 (17)
O(1)	468 (18)	229 (14)	520 (20)	−134 (24)	−170 (27)	−25 (28)
O(2)	1170 (38)	743 (32)	949 (36)	1304 (59)	968 (57)	1647 (64)
O(3)	357 (15)	507 (19)	227 (13)	−56 (26)	296 (26)	120 (21)
O(4)	1273 (39)	586 (27)	605 (27)	−1030 (53)	485 (44)	−1325 (54)

Table 1 (*cont.*)

(*c*) Coordinates of the hydrogen atoms (× 10⁴) and parameters B(in Å²) for crystal 2

	x	y	z	B
H(1)	338 (3)	87 (4)	112 (2)	0·4 (6)
H(2)	203 (3)	−86 (4)	−97 (2)	1·0 (7)
H(3)	364 (4)	39 (5)	−89 (2)	2·6 (10)
H(4)	177 (3)	−47 (4)	109 (2)	1·0 (7)
H(5)	492 (4)	178 (5)	111 (2)	2·1 (9)
H(6)	571 (3)	275 (4)	77 (2)	1·2 (8)
H(7)	450 (4)	283 (5)	88 (3)	2·6 (10)
H(8)	−38 (4)	−271 (5)	−46 (3)	3·2 (11)
H(9)	−1 (4)	−138 (6)	−91 (3)	3·6 (12)
H(10)	96 (5)	−291 (6)	−74 (3)	5·0 (14)
H(11)	586 (4)	241 (5)	−38 (2)	2·3 (10)
H(12)	512 (4)	143 (6)	−83 (3)	3·9 (12)
H(13)	448 (4)	303 (6)	−62 (3)	4·0 (12)
H(14)	12 (4)	−131 (5)	93 (2)	2·5 (10)
H(15)	−47 (4)	−238 (5)	49 (2)	2·2 (9)
H(16)	54 (3)	−249 (4)	89 (2)	1·5 (8)

reflexions were given equal weight. The index R dropped to 0·093 for the 3014 reflexions of crystal 2 and to 0·103 for the 2737 reflexions of crystal 1. The final coordinates of the two refinements are equal within experimental error [Table 1(*a*)]; the standard deviations for 2 are slightly smaller than for 1. In Table 2 the F_o and F_c values of crystal 2 are compared. The intra- and inter-molecular distances and angles given in this paper are based on the average coordinates x_a, y_a, z_a given in Table 1(*a*). The analysis of the thermal motion in the next section is based on the U_{ij} values of crystal 2 [Table 1(*b*)].

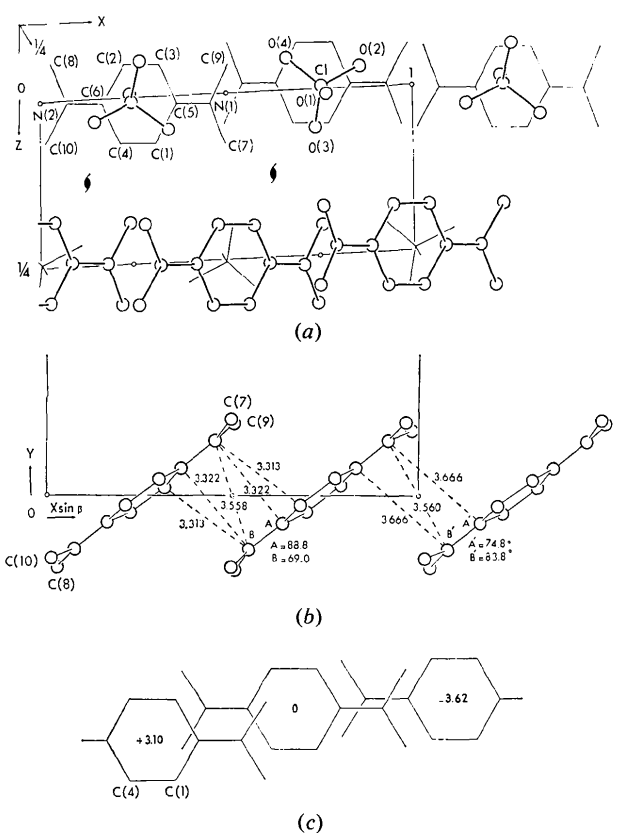

Fig. 6. Structure of TMPD.ClO_4(LT). (*a*) [010] projection. Groups around $y=\frac{1}{2}$ and around $y=0$ are drawn with bold and thin lines respectively. (*b*) [001] projection onto the a^*–b plane of three successive groups in the TMPD row along the a axis. (*c*) projection of these groups along the normal of the best plane through a benzene ring.

Analysis of the thermal parameters; disorder of the ClO_4 *group*

For the ClO_4 group, the principal axes (P, Q and R) of the temperature ellipsoids of the individual atoms are given in Table 3(*a*). We see that especially P[O(2)] and P[O(4)] are very large. It appears that P[O(2)] and P[O(4)] lie approximately in the plane defined by O(2), Cl and O(4). Their directions in this plane are given in Fig. 5. The large values obtained for the thermal parameters indicate that in the LT form the ClO_4 groups are still disordered to some extent. From Fig. 5 it can be deduced that there is rotational disorder, approximately around the axis D perpendicular to the plane through O(2), Cl and O(4). Geometrical considerations based on the model of the structure given in Fig. 6, have shown that there is space for the required large displacements of O(2) and O(4). On the basis of the X-ray experiment it cannot be decided to what extent the disorder of the ClO_4 groups is static or dynamic.

An analysis according to Pawley (1963) showed that the thermal parameters of the 'heavy' atoms of the TMPD group can be interpreted as being due to the rigid-body movement given in Table 4, $\langle[U_{ij}(o)-U_{ij}(c)]^2/\sigma^2[U_{ij}(o)]\rangle^{1/2}=1{\cdot}05$. By analogy with the results obtained for the TMPD group in TMPD.ClO_4(RT), it appears that the axes p and p' for which **T** and **ω** are largest, approximately coincide with each other and with the smallest axis of inertia of the molecule. There is no indication of disorder of the TMPD groups in the structure. It can therefore be assumed that all TMPD groups have the same electric charge, since differences in charge would result in varying orientations of the groups and thus in disorder.

Description of the structure

The [010] projection of the LT structure is given in Fig. 6(*a*). As mentioned before (see Fig. 4), the LT structure is strongly analogous to the RT structure. In both structures the TMPD groups are packed in rows which have little mutual interaction. The shortest C···C distance between different rows in TMPD.ClO_4(LT) is 3·58 Å. In the RT structure and in TMPD iodide this distance is 3·73 and 3·53 Å respectively.

Apart from the fact that in the LT structure the disorder of the ClO_4 groups is much smaller than in the RT structure, an important deviation from the RT structure is found in the stacking of the TMPD groups along **a**. Whereas the TMPD groups in TMPD iodide and in TMPD.ClO_4(RT) are equidistant (at distances of

Table 2. *Observed and calculated structure factors*

The columns are l, $|F_o|$, F_c. The values are on 10 times the absolute scale.

Table 2 (*cont.*)

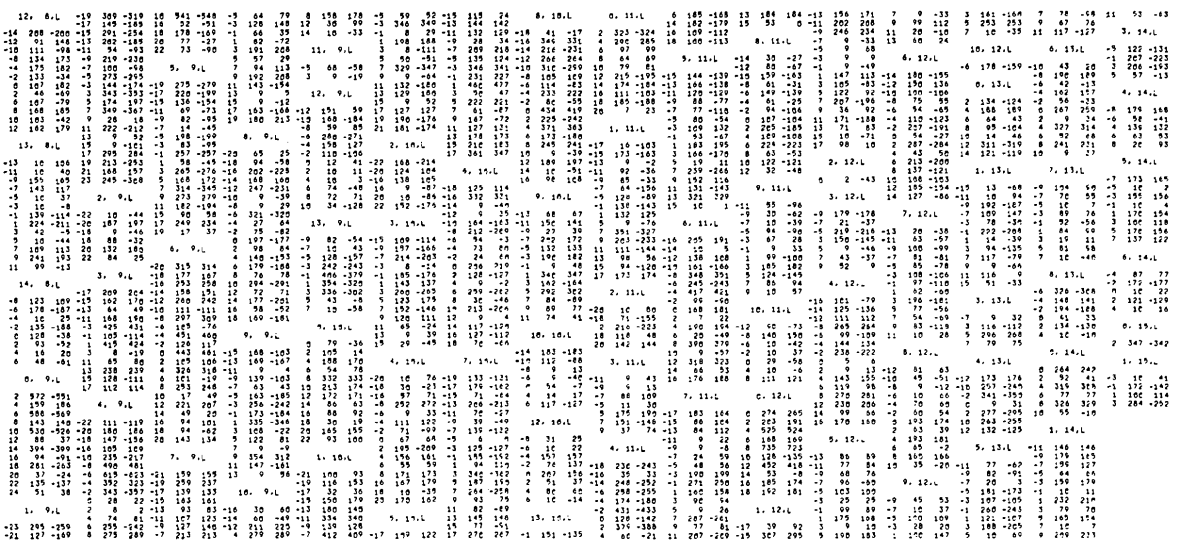

Table 3. *Vibrational parameters and geometry of the* ClO_4 *group*

(*a*) Principal axes *P*, *Q* and *R* (in 10^{-4} Å^2) with direction cosines ($\times 10^3$) relative to **a***, **b** and **c**.

P(Cl)	323	997	−63	45
Q	174	52	975	216
R	143	−58	−214	975
P[O(1)]	544	−244	−195	950
Q	484	−936	304	−178
R	188	254	933	257
P[O(2)]	2233	689	470	551
Q	352	34	−781	624
R	208	724	−411	−554
P[O(3)]	571	−40	920	389
Q	370	−971	57	−234
R	146	−238	−387	891
P[O(4)]	1989	778	−380	−501
Q	369	−131	−877	462
R	170	615	294	732

(*b*) Bond lengths and valence angles. The standard deviations are 0·002 Å and 0·2° respectively

Cl–O(1)	1·422	O(1)–Cl–O(2)	109·1
Cl–O(2)	1·414	O(1)–Cl–O(3)	110·4
Cl–O(3)	1·436	O(1)–Cl–O(4)	107·0
Cl–O(4)	1·433 Å	O(2)–Cl–O(3)	109·8
		O(2)–Cl–O(4)	110·9
		O(3)–Cl–O(4)	109·7°

Table 4. *Rigid-body analysis of the* TMPD *group*

Principal axes of the **T** (in 10^{-4} Å^2) and **ω** (in 10^{-4} rad^2) tensors with direction cosines relative to *XYZ* (*X* along **a***, *Y* and *Z* along **b** and **c** respectively). The position of the libration centre measured from the centre of gravity of the molecule is $X = 0{\cdot}24$, $Y = -0{\cdot}02$, $Z = 0{\cdot}04$ Å.

T(*p*)	177	0·803	0·597	−0·008
T(*q*)	111	−0·583	0·781	−0·224
T(*r*)	129	0·128	−0·184	−0·975
ω(*p'*)	44	0·829	0·559	−0·018
ω(*q'*)	7	−0·558	0·826	−0·083
ω(*r'*)	11	0·031	−0·079	−0·996

3·38 and 3·55 Å respectively; dBV, Fig. 2), alternating distances occur in TMPD.ClO_4(LT) [Fig. 6(*b*)]. The interplanar gaps are alternately 3·10 and 3·62 Å [Fig. 6(*c*)]. It is seen that the sidesteps in the row of molecules are largest where the interplanar distances are smallest. Owing to this the difference between the intermolecular N···N distances around (0,0,0) and $(\frac{1}{2},0,0)$ is smaller than the difference between the interplanar distances. A further reduction of the difference in N···N distances occurs due to the flexing of the molecule [Fig. 7(*a*)]. In fact we see that the sidesteps and the bending of the molecules are such that the N···N distances are equal, despite the rather unequal interplanar spacings between successive molecules in a row. The relatively large sidestep between the molecules having the smallest interplanar separation which contributes in making the N···N distances equal, causes the methyl carbon atoms C(9) and C(7) to become close to a carbon and a hydrogen atom respectively of the neighbouring molecule. Evidently because of this C(9) and C(7) are pushed far out of the benzene plane of the molecule [Fig. 7(*a*)].

In view of the discussion given above it is not surprising that the conformation of the TMPD group has changed during the phase transition. In the LT form it has lost its former 2/*m* symmetry. As is seen from Fig. 7(*b*) the reduction in symmetry is not reflected by the bond lengths and only to a slight extent by the bond angles.

The bond lengths and angles in the ClO_4 group are given in Table 4(*b*). The average Cl–O distance (1·426 Å) lies close to Sutton's (1965) value of 1·43 (2) Å, and the largest deviation of a bond angle from the tetrahedral value of 109·5° is 2·5°. Not too much significance should be attached to this deviation because of the disorder of the ClO_4 groups mentioned above.

The twinning of the crystals

As has been discussed before, the reduction in symmetry occurring during the phase transition causes twinning of the crystals. Now that both the low and room temperature structures are known, a better insight into the twinning can be obtained. Comparison of the room- and low-temperature structures given in dBV [Fig. 2(*a*)] and in Fig. 6(*b*), shows that, in rough approximation, the relative arrangement of the TMPD groups observed at room temperature is preserved in the low-temperature form for the two neighbouring groups related by the inversion centre at (0,0,0). In the discussion which follows this pair of molecules is therefore considered as a rigid unit *U* and the changes occurring in the TMPD rows during the transition are described in terms of replacements of the units *U* relative to each other. The ClO_4 ions are not considered in this paragraph. Fig. 6(*a*) shows that in the projection along the *b* axis all C(ring)–N bonds of *U* approximately lie on one line. In Fig. 8 the units are depicted schematically in [010] projection. Remember that at room temperature the N–N lines of all the molecules lie in the mirror planes perpendicular to **c**(RT). During the transition the rearrangement of the units *U* (apart from a contraction in the **a** direction which brings them closer together) can occur in two ways.

1. N–N remains perpendicular to **c**(RT) but successive units in the **a** direction show slight displacements relative to each other in the **c** direction. This is shown in Fig. 8(upper part). The sign of the shift is different for the left- and right-hand side of the Figure, which results in twinning around [001]. The two twin individuals share the **c** axis, which is a twofold axis at room temperature, and correspond with the individuals III and IV in Fig. 1.

2. The units *U* rotate over about $|90°-\beta|$ around their centre [Fig. 8(lower part)] and successive rows in the **c** direction shift along **a**, to bring **c**(LT) perpendicular to N–N. Since the sign of the rotation is different for the upper and lower parts of the Figure twinning across (001) occurs. The two individuals share the (*a*,*b*) plane, which is a symmetry plane at room temperature, and correspond with the individuals I and II in Fig. 1.

Both displacements discussed above give rise to disorder at the boundaries where twin-individuals meet. This disorder, schematically drawn in Fig. 8, is largest for the twinning around [001]. This presumably explains our observation that twinning around [001] is present to a considerably smaller extent than twinning across (001).

Discussion

The discussion on the TMPD groups given in dBV has shown that the TMPD groups in TMPD.ClO_4(LT), as well as in TMPD iodide and in TMPD.ClO_4(RT), are present as $TMPD^+$. Whereas for TMPD iodide and TMPD.ClO_4(RT) this could be anticipated from the magnetic behaviour, this is not the case for TMPD.ClO_4(LT) and therefore various proposals concerning the electric charges of the TMPD groups in TMPD.ClO_4(LT) have been made (see Introduction of dBV). The observation that the TMPD groups are present as $TMPD^+$, convincingly rules out the molionic lattice theory of Pott & Kommandeur (1967), which assumes TMPD.ClO_4(LT) to contain $TMPD^{2+}$ and TMPD°. The disproportionation mechanism proposed by Pott & Kommandeur, has also been rejected by Sakata & Nagakura (1970) on the basis of spectral data.

The marked drop in the magnetic susceptibility below the transition point must be due to some kind of coupling between the unpaired electrons on the $TMPD^+$ groups. For the way this coupling is achieved two theories are found in the literature. Firstly there is the model of Soos (1965) which is based on exchange interaction between organic radicals that are stacked in rows. This theory makes use of the Hamiltonian

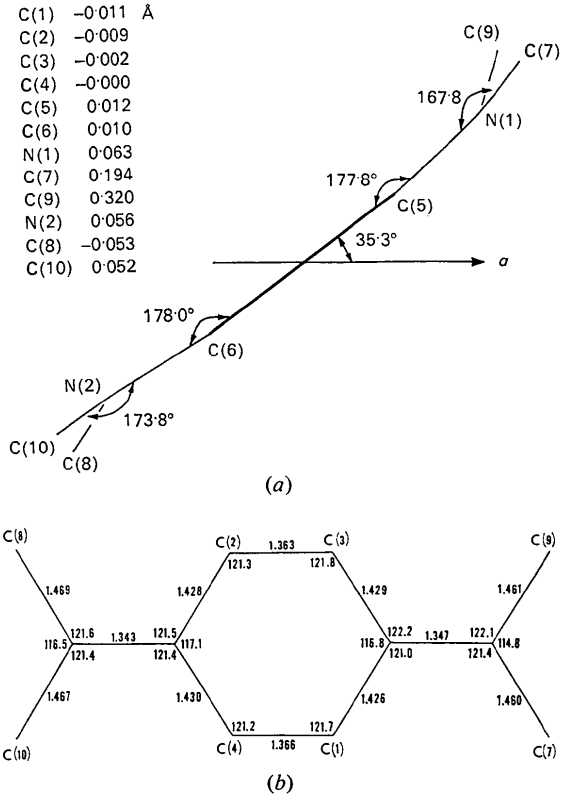

Fig. 7. The TMPD group in TMPD.ClO_4(LT). (*a*) The TMPD group seen along a line in the benzene plane perpendicular to C(5)–C(6), with distances to the best benzene plane (equation $-0{\cdot}5824X+0{\cdot}8064Y-0{\cdot}1029Z=-1{\cdot}813$ Å; see bold line). Angles between C(ring)–N bonds and adjacent planes are indicated. N(1) lies at a distance of 0·105 Å from the plane through its three surrounding C atoms, the corresponding value for N(2) is 0·053 Å. (*b*) Bond lengths and valence angles (libration corrections not applied). The calculated standard deviations for the bond lengths and angles are 0·003 Å and 0·2° respectively.

for the linear Heisenberg (anti) ferromagnet and results in a band structure for the different spin states. The exchange integral used is defined phenomenologically and includes charge-transfer effects in addition to the usual Heisenberg exchange (Soos & Hughes, 1967). The second theory, developed by Fedders & Kommandeur (1970), denies the importance of exchange effects. In this theory a 'narrow* band model' is obtained by the use of one-electron molecular orbital methods and the Bloch theorem.† Here the coupling between the electrons originates from the fact that many of them have to be placed in the same band(s).

Before applying the theories to $TMPD.ClO_4$ a comment should be made on the differences occurring between the χ values of the LT modification as reported by different authors (Pott, van Bruggen & Kommandeur, 1967, Fig. 1; Soos & Hughes, 1967, Fig. 3; this Figure is reproduced in the present paper as Fig. 9). We associate the spread in the observed χ values with our observation that the mosaic spread, especially in the LT phase, varies substantially (sometimes as much as 1·5°) from one crystal to another, indicating strong variations in the number of defects in the crystals. Moreover distinct differences in the twinning of the crystals appeared to occur. That the magnetic properties of the crystals depend on their twinning was confirmed by the finding that crystals showing complex twinning have a relatively high paramagnetism at low temperature. The magnetic measurements were made by Vegter (1968). We are therefore inclined to ascribe the discrepancies between the experimental χ curves below the transition point to imperfections which are presumably not of a chemical but of a crystallographic nature, and expect that the relatively high χ values measured by Duffy (1962) are obtained from relatively imperfect crystals.

* To be understood as narrow compared with band widths in metals.

† A similar description has recently been given by Strebel & Soos (1970) for aromatic donor–acceptor crystals containing rows in which *D* and *A* molecules alternate.

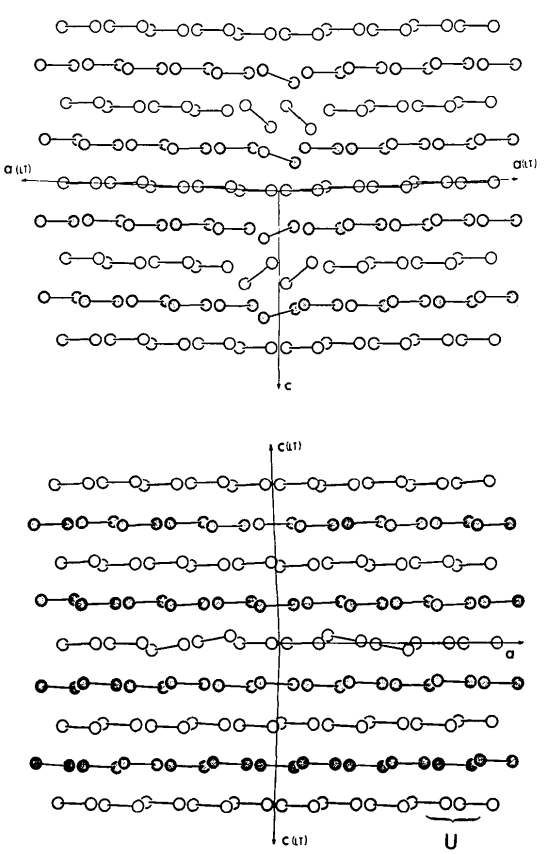

Fig. 8. Schematic representation of the twinning. Upper part: around [001]. Lower part: across (001). Neighbouring TMPD groups related *via* the inversion centre (0,0,0) [see Fig. 7(*a*)] are represented as a unit *U*. The circles correspond with the positions of the nitrogen atoms. Shaded groups lie athwart $y=\frac{1}{2}$ and unshaded ones at $y=0$.

Fig. 9 shows that application of Soos's theory to $TMPD.ClO_4$ gives good agreement between calculated and experimental χ values. It must be noticed that for the low-temperature range a still better fit can be achieved by assuming that the exchange integral J increases with decreasing temperature as this gives the calculated curve a steeper slope. That such an assumption is reasonable can be deduced from the experiments of Sakata & Nagakura (1969) who observed a large increase of the intensity of the charge transfer band with decreasing temperature. This suggests that, conditioned by gradual structural changes, the interaction between the radicals, and therefore J, increases with decreasing temperature.

When applying the theory of Fedders & Kommandeur (FK) we made use of the overlap integrals calculated by Tanaka & Mizuno (1969) and the transfer integrals (for definition, see FK, 1970) calculated by van Zorge (1970). From these integrals we estimated the width of the one band occurring in the room-temperature phase at $E_w/k=570$°K. In the LT modification there are, because of the alternation in the rows, two bands. For each band a width $E_b/k=575$°K was calculated, whereas for the band gap the value $E_g/k=2300$°K was found for the crystal structure determined at 110°K. When explaining the observed $\chi(T)$ curve with these values difficulties arise, however. Firstly, although the large LT band gap does explain the steep slope in the $\chi(T)$ curve, it is not in accordance with the fact that its value is as high as approximately 6×10^{-4} e.m.u./mol. Secondly, the χ values of the RT form obey the Curie–Weiss relation $\chi=C_0/(T+36)$ (Duffy, 1962), indicating that in this modification the coupling between the electrons on the $TMPD^+$ groups is small, which is not expected for a band having a width large in comparison with the temperature (570°K compared with $186<T<300$°K). In agreement with FK, one could enhance the susceptibility by assuming that the band is disturbed by irregularities due to the lattice vibrations, but it is not reasonable to assume that the

vibrations in the considered temperature range would destroy a band of width 570° almost completely.

From the discussion given above we conclude that the theory given by Soos is much more appropriate to explain the $\chi(T)$ curve of TMPD.ClO_4 than the theory of Fedders & Kommandeur. This is not surprising, since electron spin resonance experiments by Thomas, Keller & McConnell (1963) have shown that the exchange interaction in TMPD.ClO_4, neglected in the narrow-band model, is considerable (the singlet-triplet separation is 246 ± 20 cm^{-1}). On the other hand, the narrow-band model gives the best results for compounds like DPPH (diphenylpicrylhydrazyl) or PAC (picrylaminocarbazyl) for which the exchange interaction is small (Pake, 1962). It would be interesting to know whether the assumption of the theory that the organic radicals are arranged in rows, holds for DPPH and PAC. Structure investigations of these compounds by X-ray diffraction are, therefore, being made in our laboratory.

The authors thank Professor Kommandeur, Professor Nieuwpoort and Dr J. G. Vegter for valuable discussions. We are grateful to Dr R. B. Helmholdt for his contribution to the computer programs necessary to interpret the intensity data and to Dr B. C. van Zorge for performing theoretical calculations. All computations were done with the kind assistance of the staff in the Computing Centre of the University of Groningen.

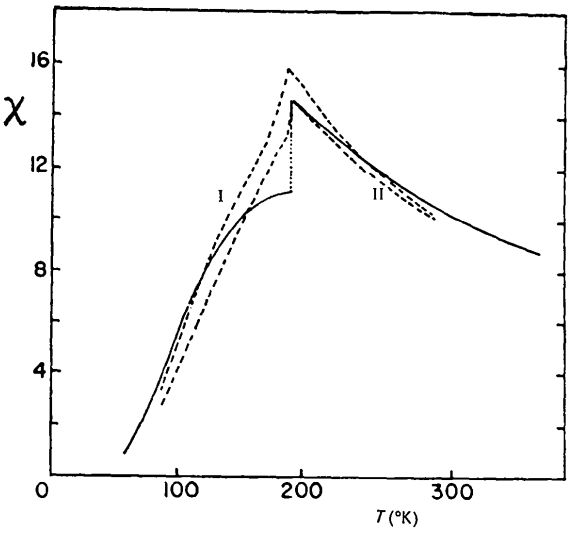

Fig. 9. Paramagnetic susceptibility χ of TMPD.ClO_4 (in 10^{-4} e.m.u./mol; reproduced from Soos & Hughes, 1967). The experimental values of Duffy (1962) and Okumura (1963) are represented by curve I and curve II respectively. The full line is calculated by Soos with $J(LT) = 132$ cm^{-1}, $\delta(LT) = 0{\cdot}75$ and $J(RT) = 139$ cm^{-1}.

References

Boer, J. L. de & Vos, A. (1972). *Acta Cryst.* B**28**, 835.

Bolhuis, F. van (1971). *J. Appl. Cryst.* **4**, 263.

Doyle, P. A. & Turner, P. S. (1968). *Acta Cryst.* A**24**, 390.

Duffy, W. (1962). *J. Chem. Phys.* **36**, 490.

Fedders, P. A. & Kommandeur, J. (1970). *J. Chem. Phys.* **52**, 2014.

Okumura, K. (1963). *J. Phys. Soc. Japan*, **18**, 69.

Pake, G. E. (1962). *Paramagnetic Resonance*. New York: Benjamin.

Pawley, G. S. (1963). *Acta Cryst.* **16**, 1204.

Pott, G. T., Bruggen, C. F. van & Kommandeur, J. (1967). *J. Chem. Phys.* **47**, 408.

Pott, G. T. & Kommandeur, J. (1967). *J. Chem. Phys.* **47**, 395.

Sakata, T. & Nagakura, S. (1969). *Bull. Chem. Soc. Japan*, **42**, 1497.

Sakata, T. & Nagakura, S. (1970). *Mol. Phys.* **19**, 321.

Soos, Z. G. (1965). *J. Chem. Phys.* **43**, 1121.

Soos, Z. G. & Hughes, R. C. (1967). *J. Chem. Phys.* **46**, 253.

Stewart, R. F., Davidson, E. R. & Simpson, W. T. (1965). *J. Chem. Phys.* **42**, 3175.

Strebel, P. J. & Soos, Z. G. (1970). *J. Chem. Phys.* **53**, 4077.

Sutton, L. E. (1965). *Tables of Interatomic Distances and Configuration in Molecules and Ions*, Supplement 1956–1959. London: The Chemical Society.

Vegter, J. G. (1968). Private communication.

Tanaka, J. & Mizuno, M. (1969). *Bull. Chem. Soc. Japan*, **42**, 1841.

Thomas, D. D., Keller, H. & McConnell, H. M. (1963). *J. Chem. Phys.* **39**, 2321.

Zorge, B. C. van (1970). Private communication.